Near-band gap electronic structure of the tetragonal rare-earth cuprates R_2CuO_4 and the bismuth cuprate Bi_2CuO_4

R. V. Pisarev,[1] V. V. Pavlov,[1] A. M. Kalashnikova,[1,2] and A. S. Moskvin[3]

[1]*Ioffe Physical-Technical Institute, Russian Academy of Sciences, 194021 Saint Petersburg, Russia*

[2]*Institute for Molecules and Materials, Radboud University Nijmegen, 6525AJ Nijmegen, The Netherlands*

[3]*Ural State University, 620083 Ekaterinburg, Russia*

(Received 16 July 2010; published 1 December 2010)

Complex optical dielectric function in the tetragonal rare-earth cuprates R_2CuO_4 (R=La, Pr, Nd, and Sm) and in the tetragonal bismuth cuprate Bi_2CuO_4 is studied in the spectral range of 0.6–5.4 eV using a method of optical ellipsometry. The dielectric spectra are studied for the two main polarizations and analyzed in terms of a cluster model for CuO_4^{6-} complexes taking into account intracenter p-d and intercenter d-d charge-transfer (CT) transitions. The band gap in the rare-earth cuprates is defined by an electric-dipole-allowed CT transitions centered at 1.54–1.59 eV in Pr, Nd, and Sm cuprates, and 2.1 eV in La cuprate. Optical response of Bi_2CuO_4 strongly differs from the rare-earth cuprates which we relate with strong covalency of Bi-O bonding and strong ionicity of Cu($3d$)-O($2p$) bonding. These features are manifested in suppression of low-energy intense intracenter p-d and intercenter d-d CT transitions, and by appearance of strong intense absorption bands near 5 eV. Regardless the strong distinctions of optical response, on one hand, of La, Pr, Nd, and Sm cuprates, and on the other hand, of the Bi cuprate, the dielectric gap in these compounds shows comparable values defined by a superposition of intracenter p-d CT transitions and two-center d-d CT transitions. Thus these cuprates should be classified as compounds intermediate between CT and Mott-Hubbard insulators.

I. INTRODUCTION

Copper compounds with the general chemical formula R_2CuO_4, where R are rare-earth ions and Bi, are a family of strongly correlated complex $3d$ oxides which raised a strong interest after discovery of high-T_c superconductivity in hole-doped La_2CuO_4,[1] and in electron-doped Nd_2CuO_4.[2] During last years these and relevant compounds have been actively studied.[3] Interestingly, the superconductivity was recently achieved in T'-R_2CuO_4 thin films with T_C substantially higher than in "electron-doped" analogs.[4] Nevertheless problems of electronic states and nature of particular physical and chemical properties of strongly correlated cuprates remain actively discussed.

The nature of the low-energy optical electron-hole excitations in the $3d$-metal oxides is an important challenging issue for the strongly correlated systems. These excitations are important because they play a central role in multiband Hubbard models used for describing both the insulating states as well as the unconventional states which emerge under electron or hole doping. One of the key problems in the physics of oxygen cuprates is the relation between their near-band gap electronic structure and the local oxygen coordination of the Jahn-Teller $Cu^{2+}(3d^9)$ ions. Furthermore, the interaction between Cu-O clusters is a factor which strongly influences the electronic structure. Tetragonal cuprates R_2CuO_4 and Bi_2CuO_4 provide an interesting opportunity to address this problem. The point is that the crystal structure of tetragonal R_2CuO_4 cuprates varies from the so called T phase [Fig. 1(a)] with strongly distorted octahedral CuO_6^{10-} complexes for the cuprates with large ionic radius (R=La) to the T' phase [Fig. 1(b)] for the cuprates with smaller ionic radius (R=Pr, Nd, Sm) where the key elements are the planar CuO_4^{6-} complexes. Quasi-two-dimensional (2D) character of

copper-oxygen bondings defines many physical properties of cuprates such as strong anisotropy of magnetic, optical, and other properties, as well as the superconductivity in doped cuprates.

Though the ionic radii of Bi^{3+} and the rare-earth ions R^{3+} (R=La, Pr, Nd, and Sm) for the coordination number 8 are close to each other[6] their electronic structure is noticeably different. The $4f$ shell in the bismuth atom is fully filled. The presence of $6s$ and $6p$ electrons and resulting strong covalency of the Bi($6s,6p$)-O($2p$) bonding leads to important differences between the crystallographic and electronic structure of bismuth cuprate, and the rare-earth cuprates. In the La cuprate (space group $Abma$, T-phase) copper ions are placed in tetragonally distorted octahedral positions with three-dimensional (3D) couplings between them [Fig. 1(a)]. In Pr, Nd, and Sm cuprates (space group $I4/mmm$, T' phase)[7] we are dealing with strongly coupled CuO_4^{6-} complexes sharing
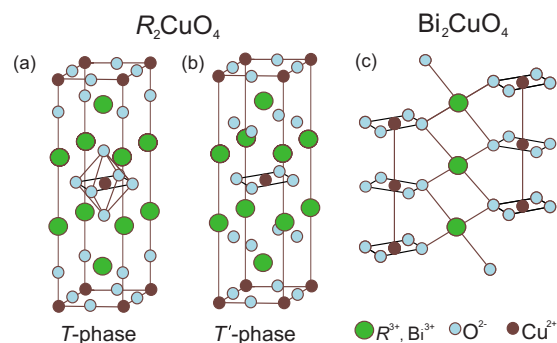

FIG. 1. (Color online) Schematic representation of the crystallographic structure of rare-earth and bismuth cuprates: (a) T phase (La cuprate), (b) T' phase (Pr, Nd, and Sm cuprates), and (c) bicuprate (after Ref. 5).

a single common oxygen ion [corner-shared (CS) coupling] thus forming well-defined CuO_2 *ab* planes. In this case the crystal structure can be regarded as 2D. By contrast, in Bi_2CuO_4 (space group $P4/ncc$) (Ref. 8) the planar CuO_4^{6-} complexes are placed one above another along the tetragonal *c* axis and the neighboring complexes are weakly coupled [see Fig. 1(c)]. In this case we can characterize the crystal structure as zero-dimensional. The strong Heisenberg exchange interaction within the CuO_2 planes in the Pr, Nd, and Sm cuprates defines 2D antiferromagnetic interaction between the spins of the Cu^{2+} ions whereas a weaker interplane interaction leads to 3D antiferromagnetic ordering in La cuprate with Neel temperatures in the range of $T_N \approx 250/320$ K.[9] Bi_2CuO_4 becomes 3D antiferromagnetically ordered at much lower temperature $T_N = 45$ K with Cu^{2+} spins oriented along the tetragonal *c* axis.[8,10,11]

Low-lying near-band gap electronic states play the most important role in defining optical and other physical properties of cuprates. In our work we report on the optical response in the rare-earth cuprates R_2CuO_4 (R = La, Pr, Nd, Sm) and in the bismuth cuprate Bi_2CuO_4. Experimental data were gained by a method of optical ellipsometry in the spectral range of 0.6/5.4 eV. The main task was to clarify the role of Cu-O complexes and the coupling between them in forming the near-band gap optical response. Spectral and polarization data for the dielectric permeability are treated in terms of a cluster model taking into account different charge-transfer (CT) transitions.

II. EXPERIMENTAL

Samples of the rare-earth and bismuth cuprates were prepared from flux-grown single crystals provided by several groups (see Acknowledgments). No intentional doping was undertaken in the process of growth implying that the obtained crystals are insulators. Nevertheless we found that the resistivity of the samples varied in a range from several kΩ (kilo-Ohms) to 200 kΩ in the rare-earth cuprates. Very high resistivity of the order of several mega-Ohm was found in the bismuth cuprate. Single crystals were x-ray oriented and cut in a form of plane-parallel plates of $\sim 1-4$ mm^2 in area with the normals along the *a* and *c* axes. Final polishing was done using a silica aqueous solution. We note that no degradation of the sample surfaces was observed over several years.

Complex dielectric functions of cuprates were studied in the range of 0.6–5.4 eV using variable-angle spectroscopic ellipsometer.[12–14] Ellipsometric angles ψ and Δ were measured at room temperature $T = 295$ K. Dielectric susceptibilities $\varepsilon^{xx} = \varepsilon^{yy}$ and ε^{zz} of optically uniaxial cuprates were calculated using the following equations:

$$\varepsilon = \sin^2 \theta + \sin^2 \theta \tan^2 \theta \left(\frac{1 - \tan \psi e^{i\Delta}}{1 + \tan \psi e^{i\Delta}} \right)^2, \quad (1)$$

where θ is the angle of incidence of the light beam.

The chosen sample orientations allowed us to derive pseudodielectric functions both along and perpendicular to the optical axis of uniaxial crystals.[15] We note that the measurements were done at several, typically three, angles of
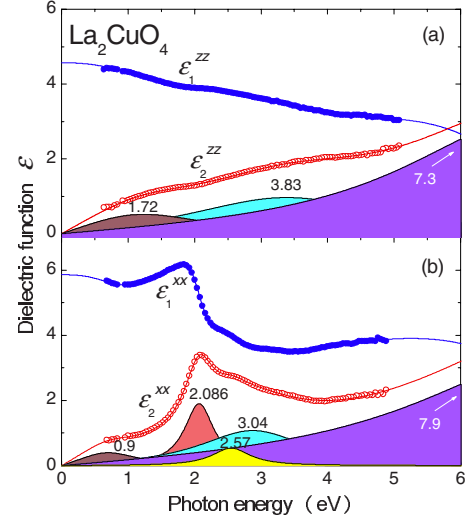

FIG. 2. (Color online) Spectra of real ε_1 and imaginary ε_2 parts of the optical dielectric function in La_2CuO_4. Color-shaded areas show single oscillators obtained by fitting experimental data according to Eq. (2).

incidence and the coincidence of extracted values of dielectric constants proved the reliability of the measurements. Accuracy of the measurements and the evaluated data were limited, in particular near the borders of the spectral range, because of small sample sizes.

Since the electronic structure in cuprates can be modeled by localized states the complex optical response was analyzed with a set of Lorentzian oscillators. In this model the dielectric function $\varepsilon = \varepsilon_1 + i\varepsilon_2$ can be presented in a following form:

$$\varepsilon = A + BE + \sum_n \frac{f_n}{E_n^2 - E^2 - iE\gamma_n}, \quad (2)$$

where A and B are coefficients describing contributions of particular transitions beyond the spectral range of measurements; E_n are resonance energy of oscillators; f_n and γ_n are oscillator strength and relaxation parameters, respectively. Experimental data were analyzed according to Eq. (2) with a use of a FORTRAN program which allowed us to make simultaneous fitting of both real ε_1 and imaginary ε_2 parts of the dielectric function.

III. EXPERIMENTAL RESULTS

Figure 2 shows optical real ε_1 and imaginary ε_2 parts of dielectric spectra for the La cuprate and Figs. 3–5 show the similar data for the Pr, Nd, and Sm cuprates. For the La, Pr, and Sm cuprates the spectra are given for both main polarizations $\varepsilon^{xx}(E) = \varepsilon^{yy}(E)$ and $\varepsilon^{zz}(E)$. For the Nd cuprate only the $\varepsilon^{xx}(E)$ spectrum was measured because of the lack of samples with required orientation. One may expect the presence of crystal field *d-d* transitions between $3d$ levels split by the crystal field in the spectral range of 1.4–2.4 eV. In fact such transitions are observed, for example, in the absorption spectra of copper borate CuB_2O_4, where the fundamental absorption band gap is strongly blue shifted up to 3.8–4.0 eV.[16]
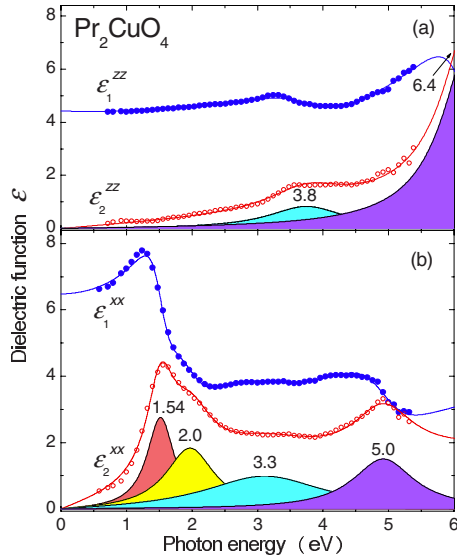
FIG. 3. (Color online) Spectra of real ε_1 and imaginary parts ε_2 of the optical dielectric function in Pr_2CuO_4. Color-shaded areas show decomposition of the spectra according to Eq. (2).

In CuB_2O_4 Cu^{2+} ions occupy both strongly distorted octahedral positions similar to La_2CuO_4 and square-planar positions similar to Pr, Nd, and Sm cuprates. However these forbidden d-d transitions are too weak to be detected in ellipsometry measurements which are sensitive only to strong transitions. Intensity and width of transitions observed in cuprates definitely allow us to assign them with charge-transfer transitions.

In their general features the spectra in Figs. 2–5 are in good agreement with known literature data obtained by reflection spectroscopy.[17–20] It is well known that ellipsometry measurements allow one to obtain more accurate data. However, to the best of our knowledge, ellipsometry measurements were done only for La and Bi cuprates.[21,22] The ellipsometry data make the decomposition of the spectra into Lorentzian oscillators according to Eq. (2) more quantitative. Lorentzians are shown by color shaded areas. Minor partial discrepancies between the data and calculations, in particular in the low-energy spectral parts, we may explain by infrared transitions[23] which were ignored in the fitting procedure.

Figure 2 shows the pseudodielectric functions spectra for T-phase cuprate La_2CuO_4, and their decomposition into
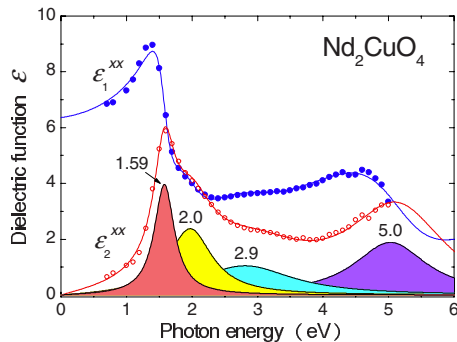

FIG. 4. (Color online) Spectra of real ε_1 and imaginary parts ε_2 of the optical dielectric function in Nd_2CuO_4. Color-shaded areas show decomposition of the spectra according to Eq. (2).

FIG. 5. (Color online) Spectra of real ε_1 and imaginary parts ε_2 of the optical dielectric function in Sm_2CuO_4. Color-shaded areas show decomposition of the spectra according to Eq. (2).

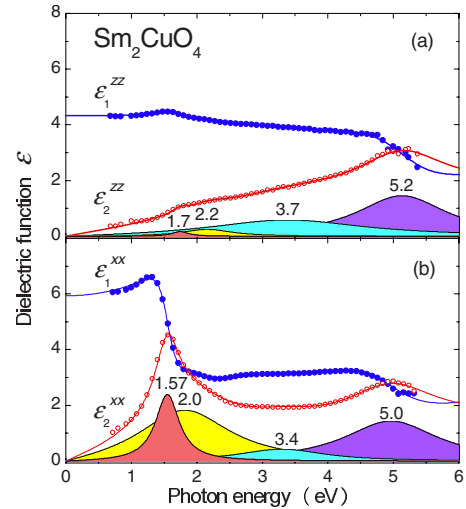Lorentzian oscillators. The characteristic spectral feature of La-cuprate spectra is a strong 2.09 eV absorption band in the $\varepsilon^{xx}(E)$ spectra which defines the band gap. We note that this band position, as well as positions of other less intensive bands at 2.57 and 3.04 eV, are in a good agreement with previously published ellipsometry data.[21]

Spectra of T' cuprates are shown in Figs. 3–5. We note, that no decomposition into Lorentz oscillators was undertaken before on the basis of reflection data[17–20] for these copper oxides. The band gap in T' cuprates is noticeably red shifted by about 0.6 eV as compared to La cuprate. As a general characterization of the spectra in Figs. 2–5 we note their strong anisotropy below 5 eV.

Figure 6 shows optical real ε_1 and imaginary ε_2 parts of dielectric spectra in Bi_2CuO_4. They are radically different from the T-phase and T'-phase cuprates. In particular we note the absence of 1.5 or 2.2 eV band, weak optical anisotropy, and dominant contribution to the optical response of high-energy transitions in the 4/5 eV spectral range. Recent paper reported the presence of an ε_2^{xx} band at about 4 eV in the bismuth cuprate.[22] However the data shown in Fig. 2 of Ref. 22 do not allow us to make more detailed comparison with our data obtained for both main polarizations and with higher resolution.

IV. DISCUSSION

For interpretation of the experimental optical spectra we shall construct an electronic energy-level diagram using a cluster model based on the hole energy spectra in the square-planar complex CuO_4^{6-}. The crystal field effects and the covalency of the Cu(3d)-O(2p) and O(2p)-O(2p) bondings will be taken into account.[24] Figure 7 shows results of calculations. We claim that our simple cluster model based on a separated CuO_4^{6-} complex has a number of advantages in comparison with, for example, band models.[25,26] These advantages are, first of all, related with involvement of correlation effects. Five 3d atomic orbitals of copper and twelve
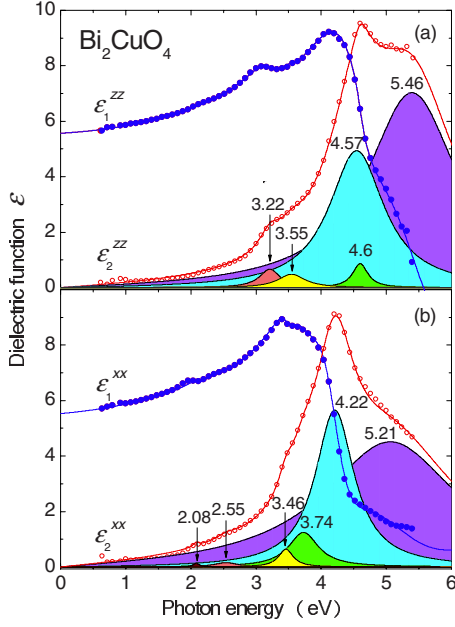
FIG. 6. (Color online) Spectra of real ε_1 and imaginary parts ε_2 of the optical dielectric function in Bi$_2$CuO$_4$. Shaded areas show decomposition of the spectra according to Eq. (2).
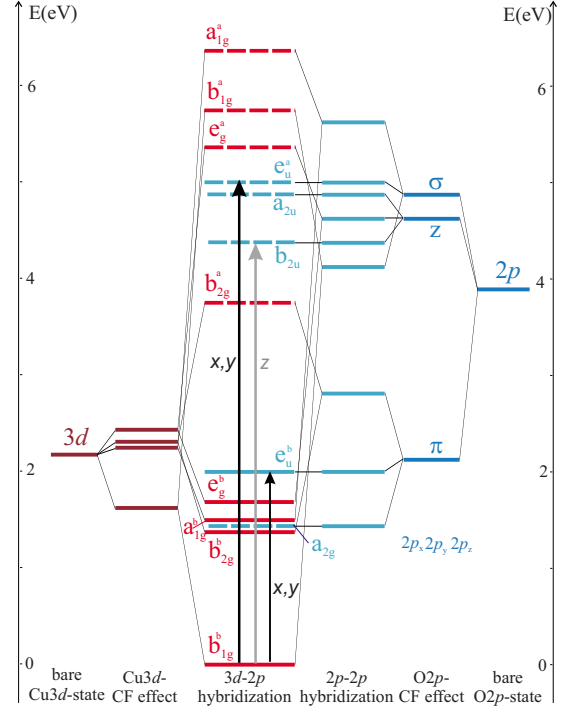

FIG. 7. (Color online) Energy spectrum of a hole in the square-planar complex CuO$_4^{6-}$. Solid and dashed lines represent bonding and antibonding orbitals, respectively. The spectrum is calculated in a cluster model taking into account crystal-field effects and covalency of Cu(3d)-O(2p) and O(2p)-O(2p) bonds. Arrows mark the most intense transitions.

$2p$ orbitals of oxygen in the CuO$_4^{6-}$ complex with the point symmetry D_{4h} form a set of even $a_{1g}, a_{2g}, b_{1g}, b_{2g}, e_g$ and odd $a_{2u}, b_{2u}, e_u(\sigma), e_u(\pi)$ molecular orbitals. The even $3d$ copper orbitals $[a_{1g}(3d_{z^2}), b_{1g}(3d_{x^2-y^2}), b_{2g}(3d_{xy}), e_g(3d_{xz}, 3d_{yz})]$ hybridize due to strong covalency of the Cu(3d)-O(2p) bonding with even O(2p) orbitals of the same symmetry. As a result, the relevant bonding γ^b and the antibonding γ^a molecular orbitals are formed. All planar O(2p) orbitals can be divided into σ orbitals $a_{1g}, b_{1g}, e_u(\sigma)$ and π orbitals $a_{2g}, b_{2g}, e_u(\pi)$, respectively. Among all odd orbitals only $e_u(\sigma)$ and $e_u(\pi)$ orbitals hybridize due to pp covalency thus forming pure oxygen bonding e_u^b and antibonding e_u^a molecular orbitals.

The pure oxygen orbitals a_{2g}, a_{2u}, b_{2u} are nonbonding. The hole energy spectrum is typical for CuO$_2$ planes in dielectric quasi-two-dimensional cuprates such as La$_2$CuO$_4$,[27] Sr(Ca)$_2$CuO$_2$Cl$_2$,[28–30] or for the CuO$_2$ chains in quasi-one-dimensional CS cuprates such as Sr$_2$CuO$_3$.[30,31]

Two electric-dipole CT p-d transitions are allowed in the CuO$_4^{6-}$ complex from the main ground state $b_{1g}^b (\propto 3d_{x^2-y^2})$ which are polarized as $\mathbf{E} \perp C_4$, $b_{1g}^b \rightarrow e_u(\pi), e_u(\sigma)$, respectively, with intensity ratio[30]

$$\frac{I(b_{1g}^b \rightarrow e_u^b)}{I(b_{1g}^b \rightarrow e_u^a)} \approx \left| \frac{t_{pp\sigma} + t_{pp\pi}}{\epsilon_{pe_u(\sigma)} - \epsilon_{pe_u(\pi)}} \right|^2, \qquad (3)$$

where $t_{pp\sigma}$ and $t_{pp\pi}$ are two types of pp transfer integrals and $\epsilon_{pe_u(\sigma)} - \epsilon_{pe_u(\pi)}$ is the energy difference of $e_u(\sigma)$ and $e_u(\pi)$ orbitals.

The relative spectral contribution of two planar CT p-d transitions is mainly defined by values of pp transfer integrals, and by the energy of $e_u(\sigma)$ and $e_u(\pi)$ orbitals. Integral intensity of two planar p-d transitions within the Cu(3d)-O(2p) bond depends on the covalency parameter

$I_{pd} \propto |t_{pd\sigma}|^2$, where $t_{pd\sigma}$ is the hole transfer integral within the Cu(3d)-O(2p) bond. We may say that the integral intensity of planar CT p-d transitions is a measure of covalency and ionicity for the Cu(3d)-O(2p) bond in CuO$_4^{6-}$ complexes. In this complex formally only $b_{1g}^b \rightarrow b_{2u}(\pi)$ transition in polarization $\mathbf{E} \| C_4$ is allowed, however the relevant matrix element is small because of the orbital orthogonality between the initial and final states.

Parity forbidden intracenter crystal field d-d transitions can be masked by more strong CT p-d transitions, first of all such as the electric-dipole-allowed $b_{1g}^b \rightarrow e_u(\pi)$ transition and the electric-dipole-forbidden $b_{1g}^b \rightarrow a_{2g}(\pi)$ transition. Most likely, the strong interaction of these states with odd-parity lattice vibrations forms a relatively broad complex absorption band near 1.5–2 eV as it was clearly observed in copper borate CuB$_2$O$_4$ where CT bands are strongly blue-shifted.[16]

Two-center CT d-d transitions in the CuO$_4^{6-}$ complex correspond to a b_{1g}-hole transfer on various states of neighboring complexes. The $b_{1g} \rightarrow b_{1g}$ transition has the lowest energy which corresponds to the formation of Cu$^{1+}(3d^{10})$ complex and the Zhang-Rice singlet with the two-hole configuration b_{1g}^2, $^1A_{1g}$ in the neighboring complex. Usually such transition is called a Mott-Hubbard transition, or, in other words, a transition to the upper Hubbard band. This transition is observed in one-dimensional and 2D cuprates with CS coupling of CuO$_4^{6-}$ complexes (Sr$_2$CuO$_2$Cl$_2$, Sr$_2$CuO$_3$) as an excitonlike band at ≈ 2.5 eV at the Γ point in the electron-energy-loss spectra (EELS) with well-defined dispersion.[30,31] A particular feature of the cuprates is well illustrated by a

complex structure of the fundamental absorption band in Sr_2CuO_3 (Ref. [31]) which is formed by overlapping of a low-energy ≈ 2.5 eV intense two-center d-d Mott-Hubbard CT transition and a relatively weak p-d one-center $b_{1g}^b \rightarrow e_u(\pi)$ CT transition at ≈ 2.0 eV.[28–31] In other words strictly speaking cuprates cannot be classified in terms of the Zaanen-Sawatzky-Allen model either as Mott-Hubbard insulators or CT insulators.[32]

Thus, in terms of the cluster model discussed above the energy spectrum of the Pr, Nd, and Sm cuprates can be associated with the charge transfer within the square-planar complexes CuO_4^{6-} (p-d CT transitions), or between the neighboring complexes (d-d CT transitions)[30,31] with properly taken into account effects of neighboring planes above and below the CuO_2 plane as well as Cu-O bond lengths.[17,18,33] Thus, important experimental observation of strong 0.6 eV "redshift" of the fundamental band gap in the Pr, Nd, and Sm cuprates (T' phase) with respect to the R=La cuprate (T phase) can be easily explained by decrease of the average negative charge in the nearest environment of CuO_4^{6-} complexes. In fact, the transition from the T-type structure to the T'-type structure leads to the energy increase of the b_{1g} hole. Taking into account these arguments we can assign the strong 1.5/1.6 eV band in the T'-cuprates to overlapping of the low-energy ≈ 2.0 eV two-center (d-d) $b_{1g} \rightarrow b_{1g}$ CT transition and the one-center (p-d) $b_{1g}^b \rightarrow e_u(\pi)$ CT transition at $\approx 1.5/1.6$ eV. It is quite natural assign absorption bands in the 3.1/3.4 eV and in the 5.0/5.2 eV spectral range (see Figs. 3–5) with a weak d-d two-center CT transition $b_{1g} \rightarrow e_u(\pi)$ and a p-d one-center CT transition $b_{1g}^b \rightarrow e_u(\sigma)$, respectively.[30,31]

We may thus conclude that the rare-earth cuprates R_2CuO_4 (R=Pr, Nd, Sm) with the T' structure, as well as other members of the cuprate family, can be assigned to insulators of intermediate class between Mott-Hubbard insulators and CT insulators. It is interesting to note that strong oscillator strength of the p-d electric-dipole-allowed $b_{1g}^b \rightarrow e_u(\pi)$ transition provided a good opportunity for observing strong resonance photoinduced optical phenomena allowing detecting of orbital and spin contributions into femtosecond dynamics in T'-type cuprates in the 1.45/1.77 eV spectral range.[34] By contrast no such phenomena were detected in T-type cuprates in the same spectral range where the band gap is by about 0.6 eV higher.

Spectra of $\varepsilon^{zz}(E)$ for the light polarization along the tetragonal axis reflect the contribution of CT transitions to the optical response. Experimental data and their decomposition into particular Lorentz oscillators show broad bands at 3.8 eV in Pr_2CuO_4 and 3.7 eV in Sm_2CuO_4 (see Figs. 3 and 5). It is quite natural to assign these bands to one-center (p-d) CT transition $b_{1g}^b \rightarrow b_{2u}$. In Sm_2CuO_4 (Fig. 5) two more week bands can be distinguished at 1.7 and 2.2 eV, which can be attributed to forbidden transitions and/or to a small buckling of CuO_4^{6-} complexes from the ab planes. High-energy bands in the $\varepsilon^{zz}(E)$ spectra at 6.4 eV in Pr_2CuO_4 and at 5.2 eV in Sm_2CuO_4 show significant difference both in the band position and intensity. That may be a hint to the rare-earth-ion contribution, for example due to a CT transition $O(2p)-R(6p)$. Indirect evidence of charge transfer from the oxygen to the rare-earth ions within the CuO_2 planes is a de-crease in the intensity of a usually strong p-d CT transition $b_{1g}^b \rightarrow e_u(\sigma)$.

The optical response of the bismuth cuprate Bi_2CuO_4 shown in Fig. 6 radically differs from the response of the T'-type cuprates (see Figs. 3–5). First of all we note unexpectedly small anisotropy. The response of Bi_2CuO_4 is strongly suppressed in the low-energy spectral range. By contrast the high-energy response is increased. On the other hand the optical response of Bi_2CuO_4 in general features is in agreement with the EELS results[35] and with local density approximation calculations which point to a dominant contribution of the Bi-O subsystem.[36] Intense ε_2 bands at 4.57 and 5.46 eV in z-polarization and at 4.22 and 5.21 eV in x polarization correspond to a double-band feature in the EELS spectrum at 4.4/6.1 (B' structure).[35] These bands are attributed to transitions from hybridized bonding and antibonding $Bi(6s)$-$O(2p)$ orbitals in the Bi_2CuO_4 valence band into empty $Bi(6p)$ states.[35] Strong covalency of $Bi(6s, 6p)$-$O(2p)$ bonds leads to increase of ionicity within the $Cu(3d)$-$O(2p)$ bonds[35] thus suppressing spectral weight of both p-d and d-d CT transitions. We note that similar to Bi_2CuO_4, strong covalency of Bi-O bonds also leads to noticeable increase in the optical response in a prominent multiferroic bismuth ferrite $BiFeO_3$.[37]

Nevertheless, the Bi_2CuO_4 spectra in the x polarization allow us to distinguish several weak bands at 2.08 eV, 2.55 eV, 3.46 eV, and 3.74 eV which, as in the case of the rare-earth cuprates, can be attributed to a p-d intracenter $b_{1g}^b \rightarrow e_u(\pi)$ CT transition, d-d intercenter $b_{1g}^b \rightarrow b_{1g}^b$ CT transitions, and a p-d intracenter $b_{1g}^b \rightarrow e_u(\sigma)$ CT transition, respectively. The last one, presumably, is hidden within the intense Bi-O band. Two z-polarized spectral features at 3.22 and 3.55 eV can be attributed to a p-d one-center $b_{1g}^b \rightarrow b_{2u}$ CT transition and additionally to contributions of in-plane transitions due to a small buckling of CuO_4^{6-} complexes from the ab plane.

Before concluding the discussion of the R_2CuO_4 cuprates we would like to make following remarks. Recently it was found that lithium cuprate $LiCu_2O_2$, where Cu^{2+} ions occupy square-planar positions similar to those in Pr, Nd, and Sm cuprates, demonstrates anomalous optical absorption spectra.[38,39] The optical response of $LiCu_2O_2$ is characterized by an extremely strong, sharp, and highly anisotropic optical feature at 3.27 eV whereas low-energy 1.6–2.1 eV features seen in R_2CuO_4 cuprates are suppressed. An exciton-type model was suggested for explaining this feature which is based on strong electron-hole correlations and a crystal-field splitting of the Cu^{1+} states.[38]

On the other hand, it is interesting to note, that the optical CT spectra in R_2CuO_4 cuprates are qualitatively very similar to such spectra in hexagonal manganites $RMnO_3$.[13,40,41] In fact, the band gap in hexa-$RMnO_3$ is defined by a strong absorption band at 1.6 eV observed in the x polarization whereas no traces of this band are seen in the z polarization. That is very similar to Pr, Nd, and Sm cuprates with respect to both the band position and its anisotropy. We may assume that such similarity of optical CT spectra in different compounds is related to the fact that in both cases we are dealing with a single-hole state in the $3d$ shell. Mn^{3+} ion in hexa-$RMnO_3$ has the $3d^4$ state—a single hole in the half-

filled $3d^5$-shell, whereas in the Cu^{2+} cuprates we are dealing with the $3d^9$ state—a single hole in the filled $3d^{10}$ shell. In both cases the magnetic ions occupy strongly distorted uniaxial positions, namely trigonal bipyramids in the hexagonal manganites and square-planar positions in the tetragonal cuprates resulting in strong optical anisotropy with CT transitions polarized within the basal planes and strongly suppressed for perpendicular polarization.

V. CONCLUSIONS

The experimental data and their analysis on the basis of a cluster model allowed us to clarify the main features of the optical response and electronic structure of the tetragonal T-phase cuprate La_2CuO_4, the T'-type Pr, Nd, and Sm cuprates, and the bismuth cuprate Bi_2CuO_4. In-plane response $\varepsilon_{1,2}^{xx}$ in the rare-earth cuprates is weakly dependent on the type of R ion and, when the redshift is taken into account, this response is similar to those of the wide class of quasi-2D insulating cuprates where square-planar CuO_4^{6-} complexes are coupled by a common oxygen ion. Optical dielectric response is defined by contributions of one-center (p-d) and two-center (d-d) CT transitions, and the fundamental band gap is formed by their overlapping. As a result, the rare-earth cuprates may be attributed in terms of the Zaanen-Sawatzky-Allen scheme[32] to insulators of an intermediate type between Mott-Hubbard CT insulators and CT insulators. We note that the type of the R rare-earth ion strongly influence optical response in the high-energy range of 4/6 eV.

The optical response of the bismuth cuprate Bi_2CuO_4 radically differs from the response of the T-type and T'-type cuprates. Dominant contribution to the optical dielectric spectra in this compound is related to weakly anisotropic CT transitions within the Bi-O subsystem characterized by strong covalency. This factor increases the ionicity of $Cu(3d)$-$O(2p)$ bonds thus reducing the intensity of both p-d and d-d CT transitions in CuO_4^{6-} complexes. Though the intensity of these CT transitions is reduced in Bi_2CuO_4, nevertheless they are observed in the range of 2.0/3.8 eV and define the band gap in this material. Thus we conclude that the band gap in Bi_2CuO_4 is the same origin as in the R_2CuO_4 compounds.

[1] J. G. Bednorz and K. A. Müller, Z. Phys. B **64**, 189 (1986).

[2] Y. Tokura, H. Takagi, and S. Uchida, Nature (London) **337**, 345 (1989).

[3] O. Madelung, U. Rössler, and M. Schulz, *Ternary Compounds and Organic Semiconductors*, Landolt-Börnstein, New Series, Group III, Condensed Matter Vol. 41e (Springer-Verlag, Berlin, 2000).

[4] O. Matsumoto, A. Utsuki, A. Tsukada, H. Yamamoto, T. Manabe, and M. Naito, Phys. Rev. B **79**, 100508(R)(2009).

[5] J. L. García-Muñoz, J. Rodríguez-Carvajal, F. Sapiña, M. J. Sanchis, R. Ibáñez, and D. Beltrán-Porter, J. Phys.: Condens. Matter **2**, 2205 (1990).

[6] R. D. Shannon, Acta Crystallogr., Sect. A: Cryst. Phys., Diffr., Theor. Gen. Crystallogr. **32**, 751 (1976).

[7] H. Wiegelmann, I. M. Vitebsky, A. A. Stepanov, A. G. M. Jansen, and P. Wyder, Phys. Rev. B **55**, 15304 (1997).

[8] E. W. Ong, G. H. Kwei, R. A. Robinson, B. L. Ramakrishna, and R. B. Von Dreele, Phys. Rev. B **42**, 4255 (1990).

[9] R. Sachidanandam, T. Yildirim, A. B. Harris, A. Aharony, and O. Entin-Wohlman, Phys. Rev. B **56**, 260 (1997).

[10] M. Baran, Yu. P. Gaidukov, N. P. Danilova, A. V. Inushkin, A. Jedrzejczak, Yu. A. Koksharov, V. N. Nikiforov, A. Revcolevschi, R. Szymczak, and H. Szymczak, J. Magn. Magn. Mater. **196**, 532 (1999).

[11] M. J. Konstantinović, Z. Konstantinović, and Z. V. Popović, Phys. Rev. B **54**, 68 (1996).

[12] R. M. A. Assam and N. M. Bashara, *Ellipsometry and Polarized Light* (North-Holland, Amsterdam, 1977).

[13] A. M. Kalashnikova and R. V. Pisarev, JETP Lett. **78**, 143 (2003).

[14] P. A. Usachev, R. V. Pisarev, A. M. Balbashov, A. V. Kimel, A. Kirilyuk, and T. Rasing, Phys. Solid State **47**, 2292 (2005).

[15] D. E. Aspnes, J. Opt. Soc. Am. **70**, 1275 (1980).

[16] R. V. Pisarev, I. Sänger, G. A. Petrakovskii, and M. Fiebig, Phys. Rev. Lett. **93**, 037204 (2004).

[17] Y. Tokura, S. Koshihara, T. Arima, H. Takagi, S. Ishibashi, T. Ido, and S. Uchida, Phys. Rev. B **41**, 11657 (1990).

[18] T. Arima, T. Kikuchi, M. Kasuya, S. Koshihara, Y. Tokura, T. Ido, and S. Uchida, Phys. Rev. B **44**, 917 (1991).

[19] B. B. Krichevtsov, R. V. Pisarev, A. Burau, H.-J. Weber, S. N. Barilo, and D. I. Zhigunov, J. Phys.: Condens. Matter **6**, 4795 (1994).

[20] M. Ichida, K. Hayakawa, K. Matsuda, A. Nakamura, and I. Hirabayashi, Solid State Commun. **108**, 145 (1998).

[21] J. R. McBride, L. R. Miller, and W. H. Weber, Phys. Rev. B **49**, 12224 (1994).

[22] J. Kim, D. S. Ellis, H. Zhang, Y. J. Kim, J. P. Hill, F. C. Chou, T. Gog, and D. Casa, Phys. Rev. B **79**, 094525 (2009).

[23] J. D. Perkins, J. M. Graybeal, M. A. Kastner, R. J. Birgeneau, J. P. Falck, and M. Greven, Phys. Rev. Lett. **71**, 1621 (1993).

[24] A. S. Moskvin and R. V. Pisarev, Fiz. Nizk. Temp. **36**, 613 (2010) [Low Temp. Phys. **36**, 489 (2010)].

[25] H. Eskes, L. H. Tjeng, and G. A. Sawatzky, Phys. Rev. B **41**, 288 (1990).

[26] J. Ghijsen, L. H. Tjeng, J. van Elp, H. Eskes, J. Westerink, G. A. Sawatzky, and M. T. Czyzyk, Phys. Rev. B **38**, 11322 (1988).

[27] J. P. Falck, J. D. Perkins, A. Levy, M. A. Kastner, J. M. Graybeal, and R. J. Birgeneau, Phys. Rev. B **49**, 6246 (1994).

[28] H. S. Choi, Y. S. Lee, T. W. Noh, E. J. Choi, Y. Bang, and Y. J. Kim, Phys. Rev. B **60**, 4646 (1999).

[29] K. Waku, T. Katsufuji, Y. Kohsaka, T. Sasagawa, H. Takagi, H. Kishida, H. Okamoto, M. Azuma, and M. Takano, Phys. Rev. B **70**, 134501 (2004).

[30] A. S. Moskvin, R. Neudert, M. Knupfer, J. Fink, and R. Hayn, Phys. Rev. B **65**, 180512(R) (2002).

[31] A. S. Moskvin, J. Málek, M. Knupfer, R. Neudert, J. Fink, R. Hayn, S.-L. Drechsler, N. Motoyama, H. Eisaki, and S. Uchida, Phys. Rev. Lett. **91**, 037001 (2003).

[32] J. Zaanen, G. A. Sawatzky, and J. W. Allen, Phys. Rev. Lett. **55**, 418 (1985).

[33] S. L. Cooper, G. A. Thomas, A. J. Millis, P. E. Sulewski, J. Orenstein, D. H. Rapkine, S.-W. Cheong, and P. L. Trevor, Phys. Rev. B **42**, 10785 (1990).

[34] V. V. Pavlov, R. V. Pisarev, V. N. Gridnev, E. A. Zhukov, D. R. Yakovlev, and M. Bayer, Phys. Rev. Lett. **98**, 047403 (2007).

[35] A. Goldoni, U. del Pennino, F. Parmigiani, L. Sangaletti, and A. Revcolevschi, Phys. Rev. B **50**, 10435 (1994).

[36] O. Janson, R. O. Kuzian, S.-L. Drechsler, and H. Rosner, Phys. Rev. B **76**, 115119 (2007).

[37] R. V. Pisarev, A. S. Moskvin, A. M. Kalashnikova, and T. Rasing, Phys. Rev. B **79**, 235128 (2009).

[38] R. V. Pisarev, A. S. Moskvin, A. M. Kalashnikova, A. A. Bush, and T. Rasing, Phys. Rev. B **74**, 132509 (2006).

[39] M. Papagno, D. Pacilé, G. Caimi, H. Berger, L. Degiorgi, and M. Grioni, Phys. Rev. B **73**, 115120 (2006).

[40] A. B. Souchkov, J. R. Simpson, M. Quijada, H. Ishibashi, N. Hur, J. S. Ahn, S. W. Cheong, A. J. Millis, and H. D. Drew, Phys. Rev. Lett. **91**, 027203 (2003).

[41] W. S. Choi, D. G. Kim, S. S. A. Seo, S. J. Moon, D. Lee, J. H. Lee, H. S. Lee, D.-Y. Cho, Y. S. Lee, P. Murugavel, J. Yu, and T. W. Noh, Phys. Rev. B **77**, 045137 (2008).